Panagiotopoulos F., M. Shahgedanova, A. Hannachi, and D. B. Stephenson, 2003: Observed trends and teleconnections of the Siberian high: a rapidly declining centre of action. Submitted to *J. Climate*.

ABSTRACT

This study investigates variability in the intensity of the winter-time Siberian high (SH) by defining a robust SH index and correlating it with selected meteorological fields and teleconnection indices. A dramatic trend of –2.5 hPa decade^{-1} has been found in the SH between 1978 and 2001 with unprecedented (since 1871) low values of the SH. The weakening of the SH has been confirmed by analysing different historical gridded analyses and individual station observations of SLP and excluding possible effects from the conversion of station pressure to SLP. The major Northern Hemisphere teleconnection patterns explain 21% of variance in the SH index with the Arctic Oscillation and the West Pacific pattern being the most important predictors. It is suggested that a significant warming observed in Siberia over the same period is the main reason for the dramatic decline of the SH. This argument is supported by future climate projections by GCMs which predict a decline in the SH in response to projected climate change. It is also shown that the impacts of variability in the SH extend far outside its source area affecting circulation and temperature patterns in the western Eurasian Arctic and the Mediterranean particularly strongly and reaching into the equatorial western Pacific.

1. Introduction

Inspection of monthly winter sea-level pressure (SLP) maps reveals the existence of an extensive semi-permanent anticyclone over Asia. It can clearly be seen as a maximum in the winter mean SLP in the Northern Hemisphere (Fig. 1a). This feature, known as the *Siberian high* (SH), is associated with the coldest and densest air masses in the Northern Hemisphere (Lydolf, 1977). It is a semi-permanent and quasi-stationary atmospheric centre of action, dominant in the boreal winter season. The SH forms generally in October mainly in response to strong and continuous radiational cooling in the lower troposphere above the snow-covered surface of Asia and persists until around the end of April. Being primarily thermally induced, the SH is a shallow cold-core system mainly confined to the lower levels of the troposphere below the 500 hPa pressure level. The SH is usually centred over northern Mongolia but often spreads over a very large part of Asia thereby dominating low-level circulation in that area in winter (Fig. 1a).

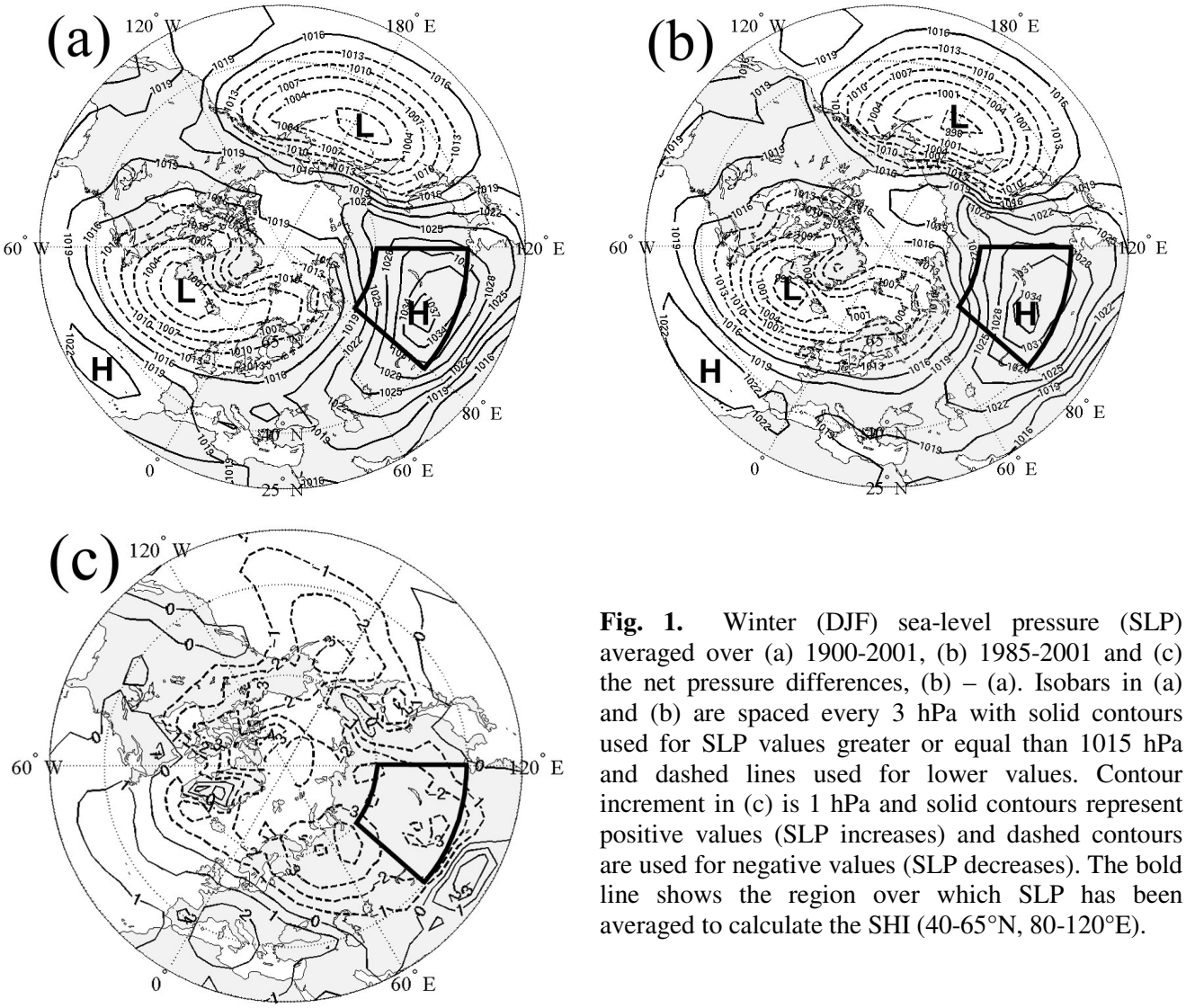

Fig. 1. Winter (DJF) sea-level pressure (SLP) averaged over (a) 1900-2001, (b) 1985-2001 and (c) the net pressure differences, (b) – (a). Isobars in (a) and (b) are spaced every 3 hPa with solid contours used for SLP values greater or equal than 1015 hPa and dashed lines used for lower values. Contour increment in (c) is 1 hPa and solid contours represent positive values (SLP increases) and dashed contours are used for negative values (SLP decreases). The bold line shows the region over which SLP has been averaged to calculate the SHI (40-65°N, 80-120°E).

Despite its prominence and large spatial extent surprisingly little is known about the temporal variability of the SH and its possible impacts on weather and climate in the Northern Hemisphere (NH). Most previous studies have tended to focus on variability in other centres of action such as the Icelandic and Aleutian lows related to the North Atlantic and North Pacific Oscillations respectively (Stephenson *et al*. 2002; Panagiotopoulos *et al*. 2002).

The few published studies on the SH are often contradictory. Sahsamanoglou *et al*. (1991) studied the climatological aspects and temporal variability of the SH by analysing a 116-year record (1873-1988) of observational SLP data compiled by Jones *et al*. (1987). Sahsamanoglou *et al*. (1991) constructed an index based on the maximum value of SLP for each month and found a gradual weakening of the SH after 1970. They related that decrease in the intensity of the SH to the continuous warming of the lower troposphere observed over Siberia during the same period. This result, however, was not confirmed by another observational study by Mokhov and Petukhov (1999) who found instead an intensification of the SH since 1960. Their study was based on SLP data derived from synoptic charts. Such data are known to contain errors, but it is not clear whether the difference in results between Sahsamanoglou *et al*. (1991) and Mokhov and Petukhov (1999) is solely due to data quality. No further research has been published on this important issue, leaving unanswered the question about the existence of any long-term trends in the intensity of the SH. Observed historical trends in the SH intensity were also not at all addressed by IPCC (2001).

The effects of the SH in weather and climate over large parts of Asia are well known and documented. Large parts of central and eastern Siberia are under the direct influence of the SH and experience extremely cold and dry conditions associated with the minimal cloud cover and the long-wave radiation losses (Lydolf, 1977). By contrast, the possible role of the SH in climatic variability over Europe and the Arctic region has received relatively little attention. Rogers (1997) studied the North Atlantic storm track variability and suggested that a westward extension of the SH into Europe is associated with a south-westerly flow and warm advection in northern Europe.

Investigation of the relationship between the SH and Eurasian snow cover has also produced inconclusive results. Clark *et al*. (1999) found no significant impact of the SH variability on temperature variability in Europe in their study of relationships between snow extent, atmospheric circulation and temperature over Eurasia. However, Cohen and Entekhabi (1999) linked changes in Eurasian snow cover extent with variability in the extent of the SH. They argued that during years with extensive autumn and winter snow cover in Eurasia, the SH expands initially westwards into northern Europe and then northwards over the frozen Arctic into North America bringing unusually cold air in these regions.

The published literature raises two important and unanswered questions: (1) what is the real trend in the intensity of the SH particularly during the last twenty years? (2) How does the SH affect weather in the extra-tropical regions of the NH and mainly in Eurasia?

This study addresses these two questions by analysing historical gridded and station monthly mean SLP data sets, which are briefly described in section 2. Temporal variability and trends in the SH intensity are discussed in section 3 and a new more reliable index of the SH (SHI) is presented. In section 4, teleconnections are investigated in the NH using the SHI and the relationship of the SHI with major teleconnection patterns is discussed. Conclusions are presented in section 5.

2. The SH index: data and methods

Because of its predominantly thermal nature and small vertical depth, the SH is best defined in terms of SLP than other fields such as 500 hPa geopotential height. This study makes use of wintertime (December to February (DJF)) means of both historical gridded analyses and individual station observations of SLP. To avoid the effect of poor interpolation due to missing data or statistical corrections applied to the data sets, three different gridded SLP data sets have been analysed and compared. All three data sets consist of monthly means of SLP and their details are summarised in Table 1.

Table 1. Details of gridded SLP data sets used in this study.

Name	Period	Resolution (Lat × Lon)	Comments
Trenberth[a]	1899-2001	5°×5°	Statistical corrections before 1922
Jones[b]	1873-2000	5°×10°	
GMSLP2[c]	1871-1994	5°×5°	A blend of observational and modelled data

a) http://dss.ucar.edu/datasets/ds010.1/ (Trenberth and Paolino, 1981).

b) http://www.cru.uea.ac.uk/cru/data/pressure.htm (Jones, 1987)

c) Available from the UK Met Office Hadley Centre (Allan *et al*. 1996)

In addition to pressure data, globally gridded monthly means of various other meteorological variables for 1948-2001 obtained from the NCEP/NCAR reanalyses have also been used (available from http://wesley.wwb.noaa.gov/reanalysis.html). Station pressure and SLP for several individual stations have also been analysed for the available data period of 1922-98. Table 2 provides information about the stations and periods with missing data.

Table 2. List of meteorological stations used in this study. All data are for 1922-1998 (available from NCAR at http://dss.ucar.edu/datasets/ds570.0/data).

Station	Location	Altitude (m)	Missing data
Barnaul	53.26°N – 83.31°E	252	1931-1941
Chita	52.05°N – 113.29°E	685	1922-1941
Enisejsk	58.27°N – 92.09°E	78	1931-1941
Erbogacen	61.16°N – 108.01°E	291	1922-1951
Irkutsk	52.16°N – 104.19°E	513	1931-1941
Kirensk	57.46°N – 108.04°E	258	1922-1941
Kolpasev	58.19°N – 82.54°E	76	1922-1951
Krasnojarsk	56.23°N – 93.17°E	194	1922-1951
Minusinsk	53.42°N – 91.42°E	254	1922-1941
Troickij Priisk	54.6°N – 113.1°E	1310	1922-1951
Turuhansk	65.47°N – 87.57°E	32	1922-1941

The reliability of the gridded data sets was tested by comparing them with station observations of SLP and surface pressure (available from NCAR). Correlations between SLP values of the gridded data sets at single grid points in the source area of the SH and observations from stations located very close to these grid points were calculated (not shown). The correlations are highest for the Hadley Centre and Trenberth data sets.

3. Temporal variability of the SH

a. Defining a SH index (SHI)

To focus on temporal variability in the source area of the anticyclone, a SH index (SHI) was computed by averaging SLP over the key region between 40-65°N and 80-120°E for each gridded data set (Fig. 1a). The geographical region was chosen by carefully preparing and examining an atlas of monthly maps of SLP for all winter months between 1871 and 2001 (392 in total, not shown). Examination of the atlas revealed that the SH dominated this area with the exception of a few months only (e.g. February 1986 and January 1971). The SH sometimes extends south of 40°N, however, this region is characterised by complex and high terrain and problems can then arise when extrapolating station pressure to SLP.

Area-averaged indices are usually more reliable and can provide more insight than single-point indices such as those used by Sahsamanoglou *et al*. (1991) and Mokhov and Petukhov (1999). This is

because of the error-averaging effect in single-point indices and because the area-averaged indices represent variability in a centre of action rather than at a single location only. To verify the area-averaged index, a station-based SHI was also constructed by taking the mean of the SLP station observations for the period 1922-98 from the eleven selected stations located within the same geographical domain (Table 2). Due to missing data, three stations were used for the period 1922-41, seven stations for the period 1922-51 and eleven stations for the period 1922-98. Indices computed by averaging data from these three groups of stations separately produced very similar results to the 11-station index presented here indicating that the number of stations used did not affect the results to any significant extent.

Winter mean (DJF) station-based SHI values were compared with the SHI estimated from the gridded data sets (Fig. 2). In general, there is very good agreement between the indices computed from the three gridded data sets which confirms their reliability. The values of the SHI based on the Trenberth and Paolino (1980) and the Hadley Centre data sets are closest to those of the station-based index (correlation coefficients are 0.93 and 0.94 respectively). By contrast, there is less agreement between the SHI derived from the Jones (1987) data set and the station-based index (r = 0.77).

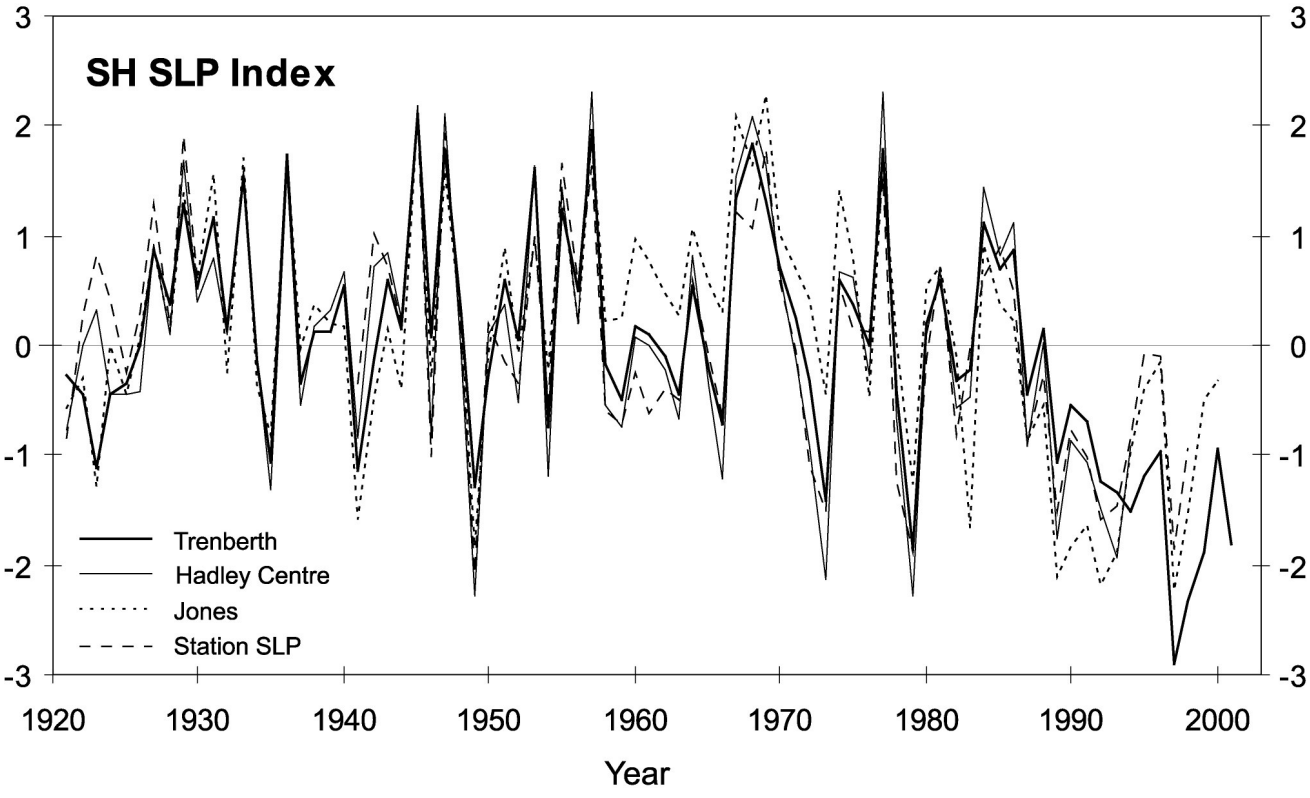

Fig. 2. Standardised winter (DJF) sea level pressure averaged over the area 40-65°N, 80-120°E using three different gridded SLP data sets and an average of observations from eleven stations within the same area in Siberia. The standard deviation is 2.1 hPa.

In addition, the Trenberth data set has a higher spatial resolution compared to the Jones data set and it is continuously updated unlike the Hadley Centre data set, which has not been updated since 1994. The Trenberth data set was chosen for further analysis on the basis of all these factors together with the fact that it is widely used in climate variability studies and many errors and discontinuities have been identified and corrected (Trenberth and Paolino, 1980). Trends and variability in the intensity of the SH were analysed using indices derived from the four data sets, however, only the index based on the Trenberth data set was used in investigation of the SH teleconnectivity.

b. Trends in the intensity of the SH

Figure 3 shows standardised DJF time series of the SHI derived from the Trenberth data set (Trenberth and Paolino, 1980). A 21-term Henderson filter is used instead of a running mean to preserve any quadratic or cubic polynomial trends in the data (Henderson, 1916). The main features of the SHI are low values at the beginning of the 20th century, higher values of SHI in the middle of the 20th century and, most importantly, a steep downward trend observed after 1977 (Fig. 3). Means were calculated and plotted for the periods 1900-77 and 1978-2001 to emphasise the different regime in the SH intensity after 1978 (Fig. 3). The steep decline of the SH after 1978 is confirmed by the SHIs derived form all four data sets (Fig. 2).

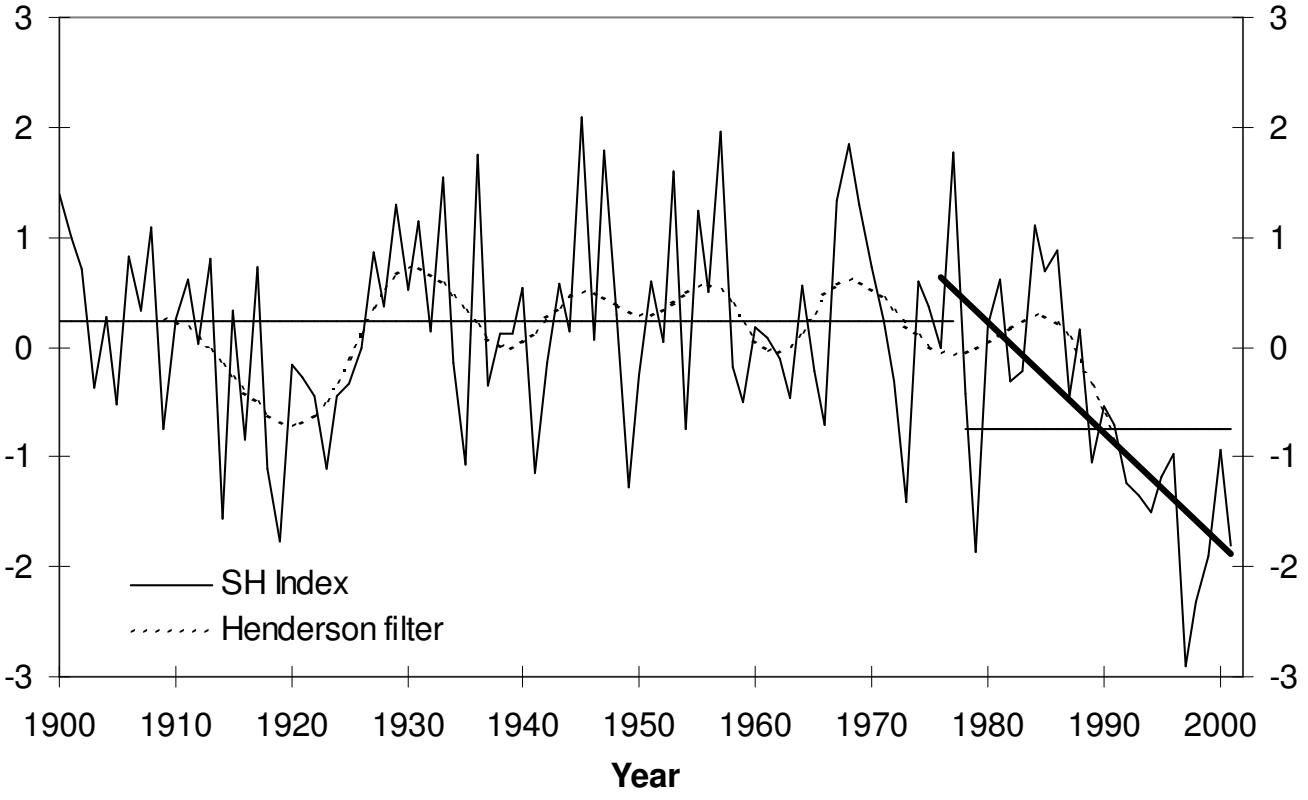

Fig. 3. Standardised winter (DJF) sea level pressure averaged over the area 40-65°N, 80-120°E using SLP data set (Trenberth and Paolino, 1981). The linear trend fit shows the decline in the SH intensity in the period 1978-2001, whereas the 10-order Henderson filter reveals the lower frequency variability. Means for 1900-77 and 1978-2001 are indicated (horizontal thin lines).

Linear regression has been used to quantify the downward trend in the period 1978-98 and also in the period 1922-98 when all four data sets were available and the results are summarised in Table 3. The mean downward trend over the period 1978-98 ranges from -1.6 hPa (decade)$^{-1}$ in the Hadley Centre and station data sets to –2.5 hPa (decade)$^{-1}$ in the Jones data set and –2.6 hPa (decade)$^{-1}$ in the Trenberth and Paolino (1980) data set. The trend is statistically significant at the 1% level in all but the Hadley Centre data set. In addition, the downward trend accounts for a large amount of total variance in the period 1978-98 reaching 41.4% for the Trenberth data. Unprecedented low values of the SHI have been observed during this period with a remarkably steep decrease in the intensity of the SH. At this rate, the SH would no longer be an anticyclonic feature by the year 2080 declining to a central pressure of 1015 hPa.

Table 3. Analysis of the SH indices derived from different SLP data sets. The p values refer to the test statistic of the null hypothesis that there is no trend in the intensity of the SH.

Data-set	Trend ± std error (hPa/decade)	p value	Variance explained (%)
1920-98			
Trenberth	-0.35 ± 0.09	<0.001	20.4
Jones	-0.31 ± 0.12	0.011	8.2
Hadley Centre	-0.16 ± 0.09	0.080	4.2
Station SLP	-0.54 ± 0.14	<0.001	21.6
1978-98			
Trenberth	-2.6 ± 0.3	<0.001	41.4
Jones	-2.5 ± 0.3	0.003	36.7
Hadley Centre	-1.6 ± 0.6	0.057	20.8
Station SLP	-1.6 ± 0.3	<0.001	31.3

The current weakening of the SH is considerably stronger than that observed at the beginning of the 20th century. The weaker mean anticyclone during the most recent 15 years can be clearly seen in Fig. 1b with the net pressure decrease over Siberia clearly visible in Fig. 1c. Compensating increases in pressure have occurred over the subtropical Atlantic and south of the Siberian high regions.

c. Possible temperature effects on the trend

The occurrence of the unprecedented downward trend in the last two decades raises questions about the origin of the trend. Trends in SLP over land must always be dealt with carefully because SLP is extrapolated from station pressure to sea-level using the hydrostatic equation, which depends on temperature. Figure 4 shows standardised DJF 2m temperature anomalies and SLP averaged over the same area as the SHI domain computed from a set of monthly mean temperatures compiled by Jones (1994) on a 5° × 5° grid. Significant warming has been observed in this area after 1970 coinciding in time with the strong weakening of the SH. A strong negative correlation of $r = -0.66$ (significantly different from zero at the 1% level) has been found between the two time series.

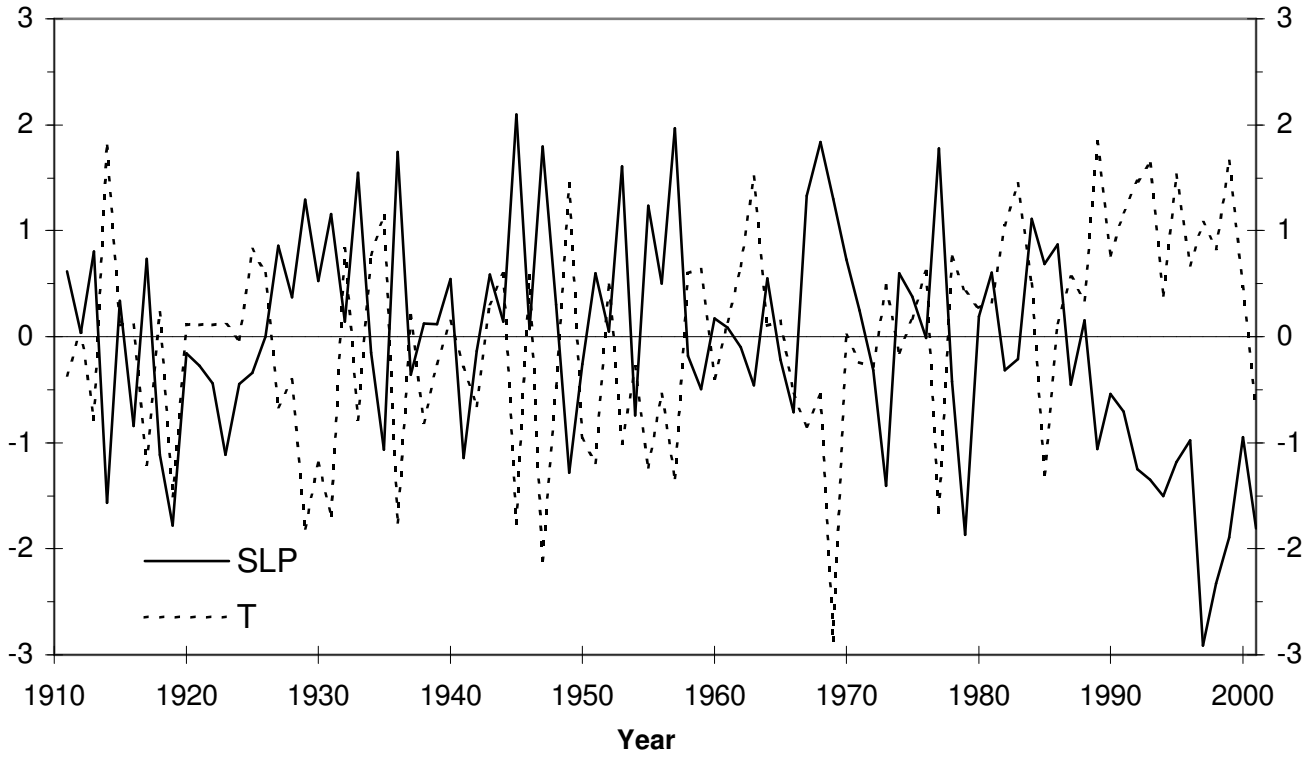

Fig. 4. Standardised winter (DJF) time series of SLP (solid curve, Trenberth and Paolino, 1980) and temperature at 2m (dashed curve, Jones, 1994) averaged over the area 40-65°N, 80-120°E. The standard deviation of (the non-standardised) SLP and temperature is 2.2 hPa and 2.02°C respectively.

Simple calculations using the hydrostatic equation, used to extrapolate pressures down to sea-level, show that even this large increase in temperature does not explain a significant decrease in SLP alone without a decrease in station pressure (see the Appendix). In particular, if there was no change in station pressure over the SHI domain during the period 1922-98, the significant rise in temperature (~3°C) observed in the area over the same period would result in a SLP decrease of only 0.6 hPa, which is significantly smaller compared to the 2.8 hPa decrease observed in SLP in the studied area.

Similar calculations for the period 1978-98 give a SLP decrease of 0.04 hPa which contrasts with the observed SLP decrease of 5.2 hPa. In fact, temperature increases of 16°C and 51°C would be required to explain alone the observed decreases in SLP over the periods 1922-98 and 1978-98 respectively, confirming that the decrease in the SH is not an artefact of the method used to compute SLP from surface pressure.

Station pressure data were also analysed for a number of individual stations (Barnaul, Chita, Enisejsk, Irkutsk, Kirensk, Minusinsk, Nerchinsky Zavod, Tomsk and Turuhansk, Table 2) and most of them also exhibit strong downward trends. Figure 5 shows the standardised DJF time series of the SHI derived by averaging SLP and station surface pressure data available from the stations within the area 40-65°N, 80-120°E for the period 1922-98. There is a very close agreement between the two indices and both exhibit low values in the last 30 years confirming the reliability of the downward trend found in the intensity of the SH.

In addition, linear trends over the periods 1900-2001 and 1978-2001 have been calculated for every grid point of the SHI domain using the Trenberth data set (not shown). The strongest trends explaining the most variance are not confined to the high terrain.

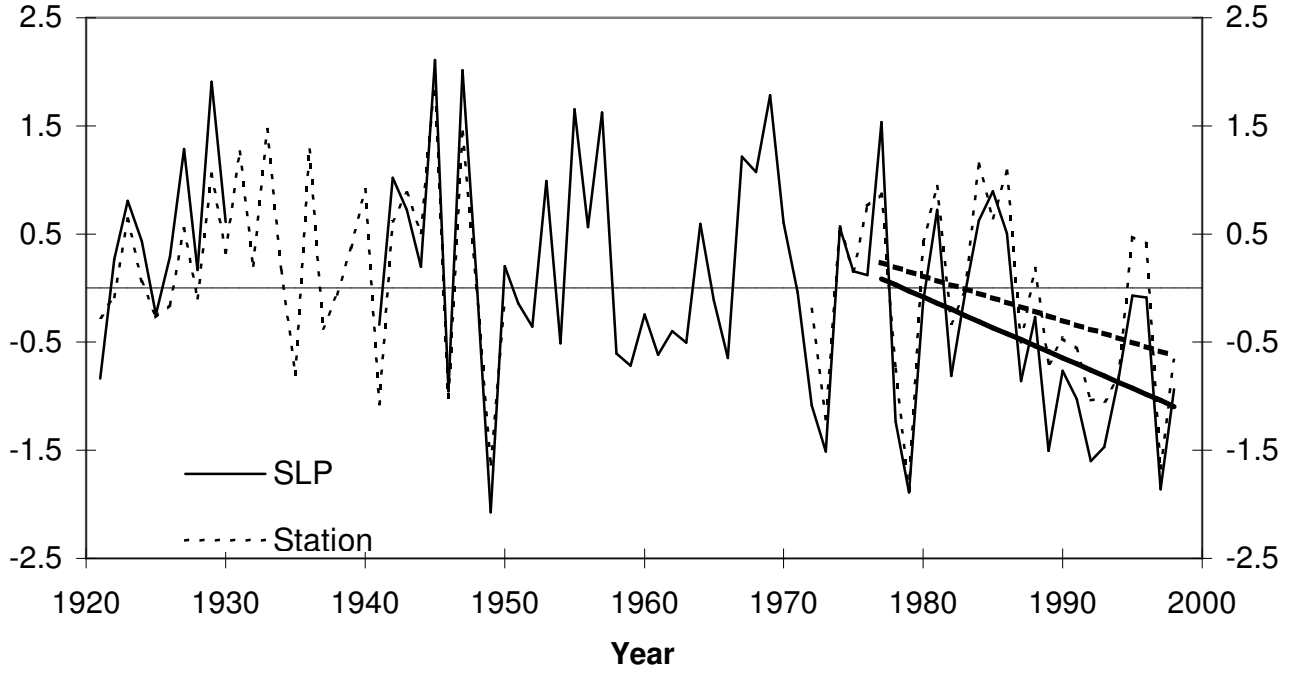

Fig. 5. Standardised winter (DJF) SLP (solid curve) and surface pressure (dashed curve) averaged using observations from station within the area 40-65°N, 80-120°E (Table 2).

d. Spatial variability in the location of the SH centre

Beside the area-averaged index of the SH constructed to study temporal variability in its intensity, the one-point technique used by Sahsamanoglou *et al*. (1991) has also been applied in this

study to analyse changes in the position of the SH centre. Figure 6 shows the time series of the geographical location (latitude and longitude) of the SH centre. The centre is defined as the grid point exhibiting the maximum SLP value over Asia for winter (DJF). Inspection of Figure 6 reveals some inter-decadal variability in north-south shift of the SH centre. During 1910-20 and 1940-50, the centre was located to the south of its normal climatological position but there is a tendency for more northerly location in recent years. Similarly, the SH centre was frequently located east of 100°E at the beginning and the middle of the 20th century, however, it has been invariably observed west of 100°E after 1960. It should be noted, however, that the movements are small compared to the large spatial scale of the SH.

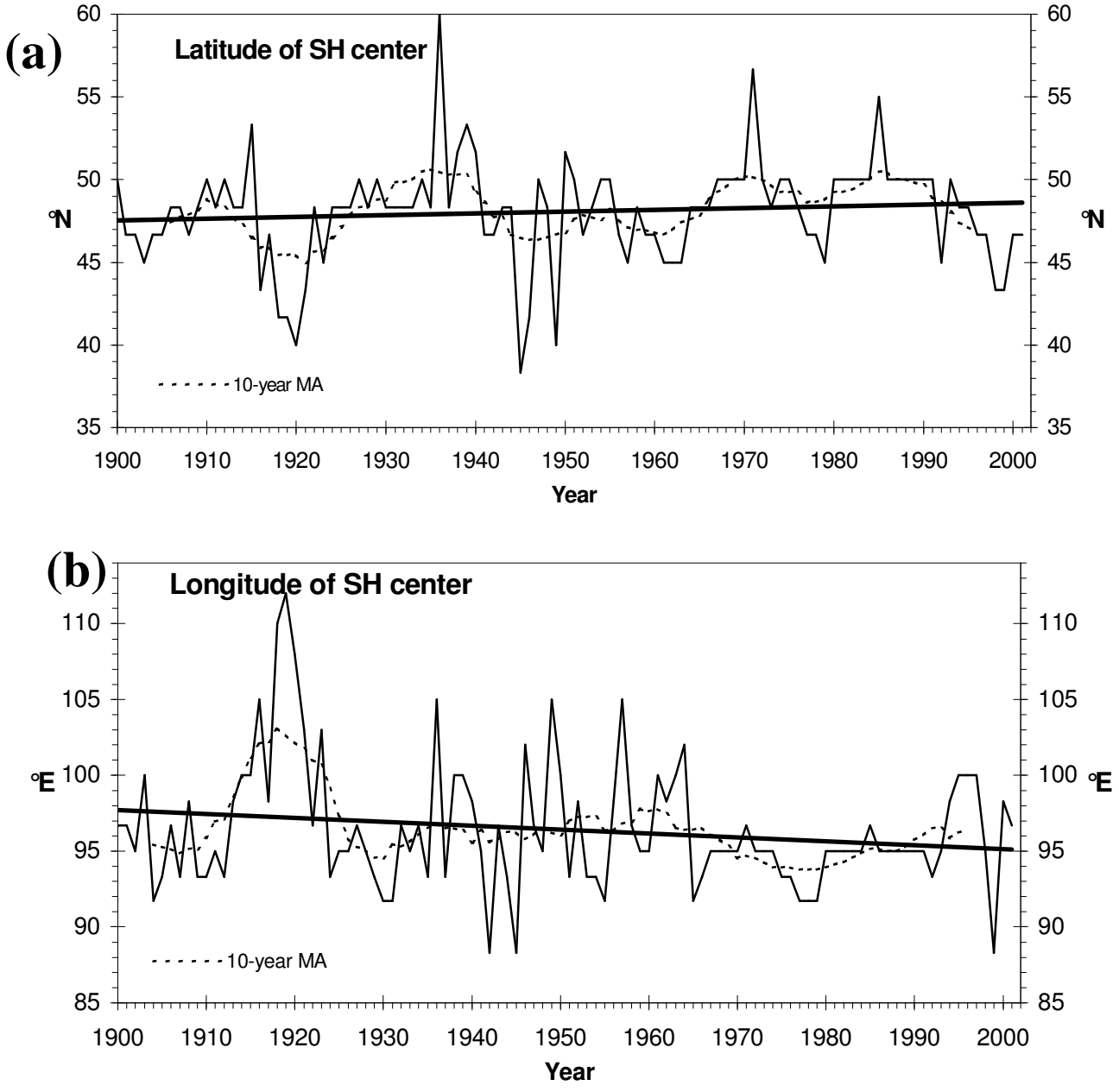

Fig. 6. Time series of (a) the mean latitude and (b) the mean longitude of the Siberian high centre taken as the maximum in the winter mean SLP over Asia (solid lines). 10-year moving averages are plotted as dashed lines.

There is a negative correlation of –0.31 (statistically significant at 5% level) between the latitude and the longitude of the SH centre implying that northern positions of the SH centre are also western ones. The location of the SH centre is related with its intensity taken as the maximum SLP value at any grid point over Asia. The correlation coefficients between the intensity of the SH and its latitude and longitude are 0.52 and -0.41 respectively and are both statistically significant at 1% level. These correlations imply that more northern and western locations of the SH centre correspond to a stronger high.

4. SH teleconnections in the Northern Hemisphere

a. Correlations between the SH index and meteorological fields

The relationships between the SH intensity and other meteorological fields have been examined by correlating the SHI derived from the Trenberth data set with this SLP field (Trenberth and Paolino, 1980) and various NCEP/NCAR reanalysis fields (Fig. 7). Linear trends have been first removed from all the fields in order to isolate interannual variability. The long-term trend in the SHI, estimated using double exponential smoothing with $\alpha = 0.78$ and $\gamma = 0.02$ (Chatfield, 2001), has been removed prior to analysis. To ensure that the correlations are not due to non-linear time trends in the data, the same correlations were also computed using backward year-to-year differences of both the SHI and the reanalysis fields producing very similar results (Fig. 8).

Figure 7a shows the correlations of the SHI with DJF averaged Trenberth gridded SLP over the period 1899-2001. As expected, an extensive area of strong positive correlations dominates northern Asia extending to southeast China. Negative correlations, statistically significant at 5% level are observed between the SHI and SLP in central Mediterranean and Libya and the subtropical part of the North Pacific. The relationship between the SH intensity and pressure over southern Europe implies that enhanced cyclogenesis over the Mediterranean is linked to positive anomalies in SH. This result is in agreement with Rogers (1997) who also linked cyclogenesis in the Mediterranean with a strong SH in his study of the North Atlantic storm track variability.

Correlations between the SHI and the zonal component of wind at 200 hPa reveal some interesting links between the SH and circulation in the upper troposphere (Fig. 7b). The subtropical jet stream over southeast China and the North Pacific is significantly stronger than usual when the SH is more intense. This intensification of the upper level winds is a characteristic feature of the East Asian winter monsoon (Cheang, 1987). The jet stream over the eastern Mediterranean Sea also intensifies with the intensification of the SH implying enhanced depression activity in this area. By contrast, the upper tropospheric zonal wind is significantly weaker over northern Asia and northern Europe. Another area of statistically significant positive correlations between the SH and upper-air zonal wind is observed in high latitudes north of the Kara Sea (80°N, 70°E). This suggests that

although the SH has largest amplitude in the lower troposphere, it has a significant non-local impact on upper-tropospheric jets and associated storm tracks on a hemispheric scale.

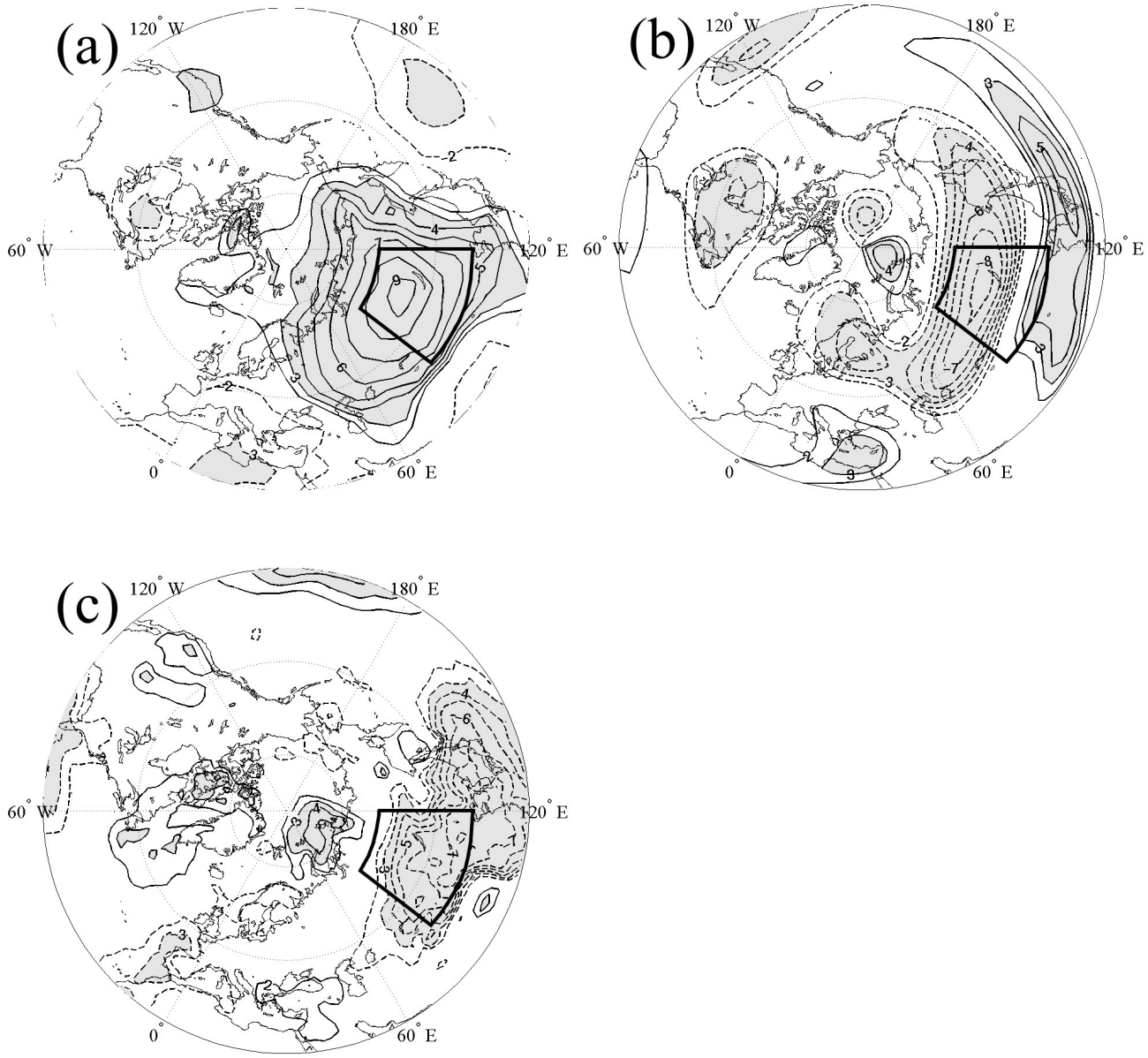

Fig. 7. Correlation map showing correlations between the SHI and (a) SLP for the period 1900-2001 (Trenberth and Paolino, 1980), (b) zonal wind (u) at 200 hPa and (c) 2m Temperature for the period 1948-2001 (NCEP/NCAR reanalysis). Correlations coefficients have been multiplied by 10. Solid contours are used for positive correlations and dashed lines for negative values. All correlations plotted in (a) are statistically significant at 5% level and grey shading is used for statistically significant correlations at 1% level ($r \geq |0.3|$). Grey shading in (b) and (c) indicates statistical significance at the 5% level ($r \geq |0.3|$).

The positive correlation between the SHI and the zonal component of the wind over the Arctic does not, however, imply that a strong SH is associated with increased storm activity in the Arctic. By contrast, increased storm activity over the last 20 years in the western (Barents, Kara and Laptev) sectors of the Eurasian Arctic has been reported by various authors. This led Rogers and Mosley-Thompson (1995) to relate milder Siberian winters to increased storminess in the Arctic and smaller spatial extent of the SH although they found no correlation between the intensity of the SH in its core

region and depression activity further north. Walsh *et al*. (1996) and Maslanik *et al*. (1996) explored changes in depression activity over the Siberian seas in relation to sea ice formation and also found strong positive trends in depression activity after 1985 when the SHI started to decline.

Further investigation of the relationship between the SHI and SLP, geopotential height and low and middle tropospheric fields of relative vorticity and vertical velocity show that the intensity of the SH is important as there is higher pressure (geopotential height) and anticyclonic conditions in this sector of the Arctic when the SH is more intense (not shown). However, a visual inspection of monthly SLP maps for all the winter months of Trenberth and Paolino data set (1980) has confirmed that spatial extent of the SH is a more important factor than the SH intensity with regard to depression activity over the Siberian seas.

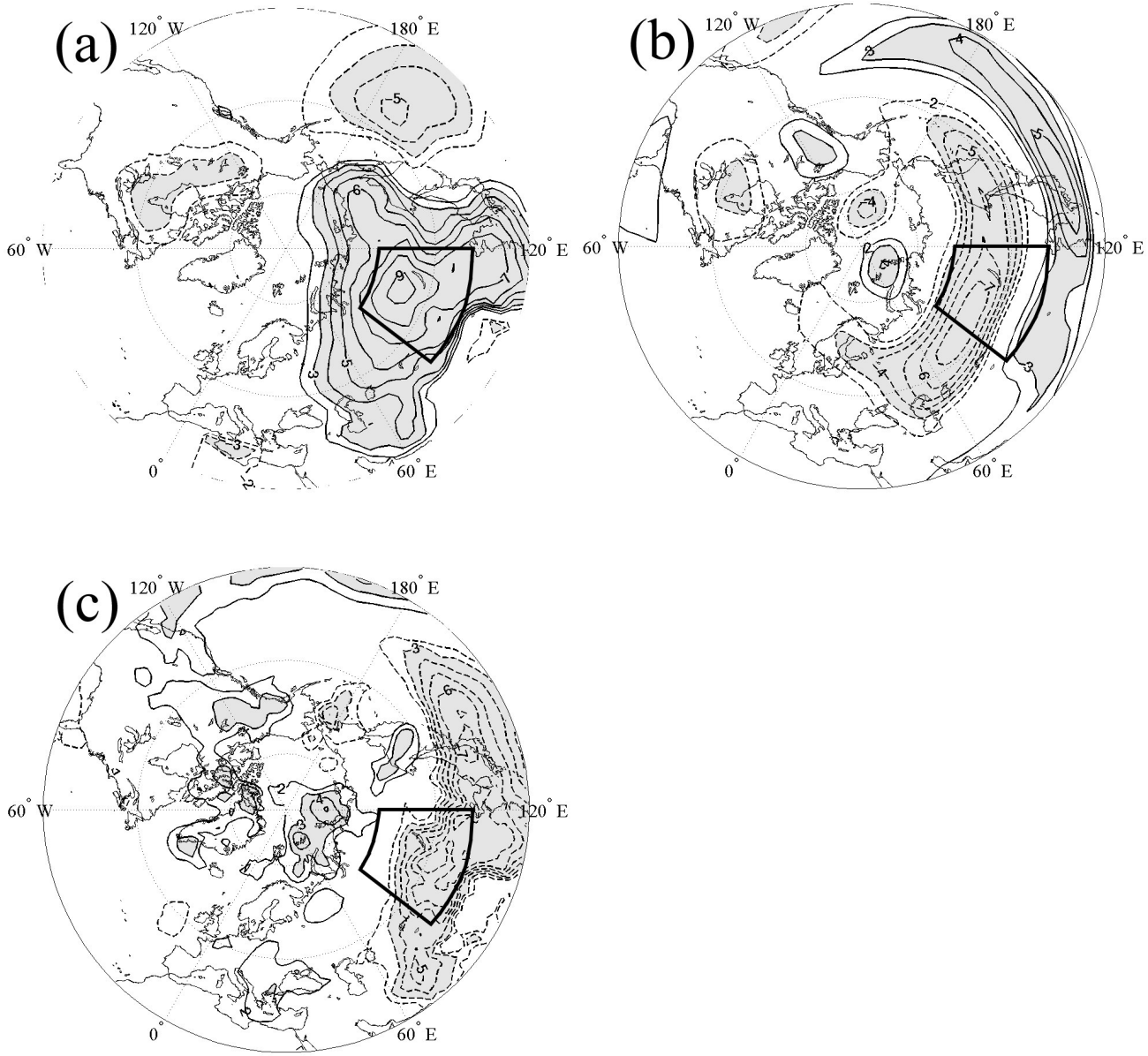

Fig. 8. Same as in Fig. 7 except for backward year-to year differences of the SHI and the fields.

Correlations between the SHI and the meridional component of wind at four different levels are shown in Fig. 9. There is clear evidence of a well-defined wave train of alternating southerly and northerly flow. The wave train is present through the depth of the troposphere with an equivalent barotropic structure but is better defined in the middle troposphere (Fig. 9b) where its extent from the subtropical North Atlantic to Central Siberia is clearly visible. Notable are strong negative correlations over Southeast Asia and the Far East at the lower troposphere (Fig. 9c and 9d) which suggest a strong link between the SH intensity and the northerly flow along the Pacific rim (the East Asian winter monsoon).

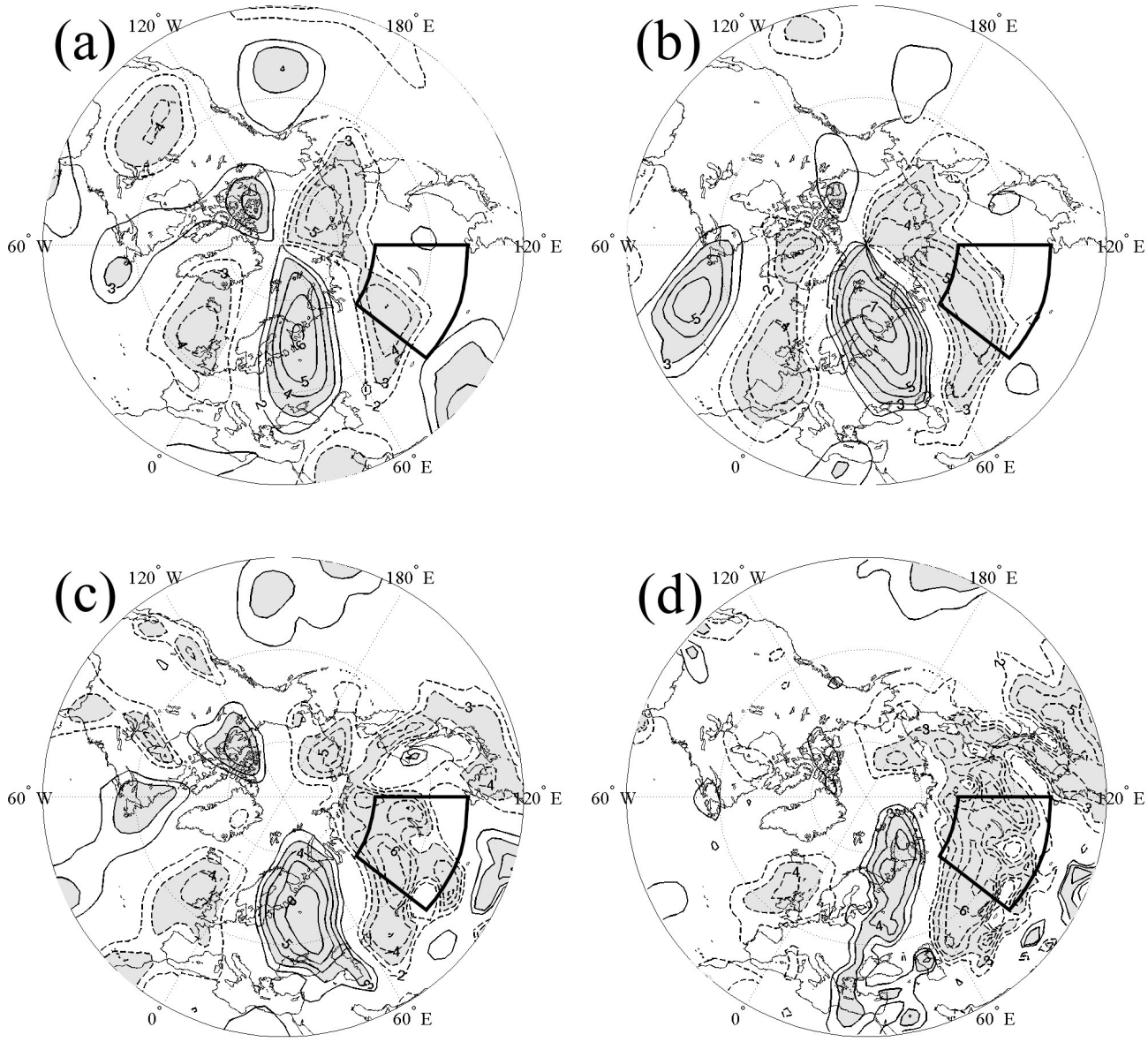

Fig. 9. Correlation map showing correlations between the Siberian high index (SHI) and the meridional component of the wind at (a) 200 hPa; (b) 500 hPa; (c) 850 hPa and (d) 2m. Correlation coefficients haven been multiplied by 10. Solid contours are used for positive correlations and dashed lines for negative values. Grey shaded contours represent correlations significant at 5% level ($r \geq | 0.3 |$).

The existence of the wave train poses a question as to whether the middle tropospheric advection affects the strength of the SH on the synoptic time scale. The existence of a similar wave train of 500 hPa geopotential height across the NH has been found to precede the onset of cold advection from Siberia to the south-east Asia (Joung and Hitchman, 1982). Lagged correlations between both monthly and 5-day means (pentads) of meridional wind at 500 hPa level and the SHI have been computed. No strong correlations have been found, which confirms that surface temperature is the most likely primary factor controlling the SH intensity.

The correlations between the SHI and air temperature (2m temperatures over land and sea surface temperatures (SSTs)) from NCEP/NCAR reanalysis are also well defined in many regions (Fig. 7c). An intense SH is associated with colder than average conditions in the SH area extending downstream to the North Pacific and Southeast Asia. This shows the profound relationship between a strong SH and the East Asian winter monsoon and the intrusions of cold air into these areas. Surges of cold air occasionally reach as far south as Malaysia according to Cheang (1977), Chiyu (1979) and Ding (1990). This analysis has found that the influence of the SH extends farther south and has a notable effect on the development of convection in the tropical Pacific. Correlation analysis between the SHI and outgoing long-wave radiation (OLR) has revealed the enhanced cloud formation between 120°E and 150°E on both sides of the Equator in association with a strong SH (not shown).

Air temperatures and SSTs in the Barents, Kara and the Laptev sectors of the Arctic exhibit positive correlations with the SH intensity. The SH affects thermal regime of the Arctic in two contrasting ways: (i) stronger than usual depression activity and advection of warm air in warm sectors of depressions is associated with weaker high while (ii) warm advection from Eastern Europe is associated with the returning south-westerly flow along the SH periphery when the SH is strong (Fig. 1a). The warming effect of the south-westerly advection is a dominant factor. This is supported by the fact that positive correlations in these areas are significantly stronger, reaching $r = 0.7$, in early winter (November and December) when the air masses over eastern Europe are still considerably warmer than the air masses over the Laptev sector of the Arctic. This effect may also explain the observed lack of warming in the Kara-Laptev sector of the Arctic despite the reported increase in depression frequency and warming projected by GCMs. While most GCMs predict that air temperatures in the Arctic should increase considerably (IPCC, 2001), no positive trends have been observed since the 1950s (Przybylak, 2000) possibly because of the reduced southerly advection associated with the currently weak SH.

The relationship between the SH and air temperature at 2m and SSTs in the Eurasian Arctic partly explains variability in the extent of sea ice particularly in the Barents-Kara sector. There is a strong negative relationship between the SHI and sea ice extent in this region (Fig. 10), which explains the reduced formation of sea ice in this region by strong warm advection from Eastern

Europe, associated with a strong SH. The impacts of the SH variability on temperature patterns in Europe are less pronounced. Southwest Europe is affected more than any other region experiencing cooler than usual conditions when the SH is strong. This is explained by stronger meridional flow and cold advection behind the more frequent low-pressure systems travelling over the Mediterranean Sea (Fig. 7a).

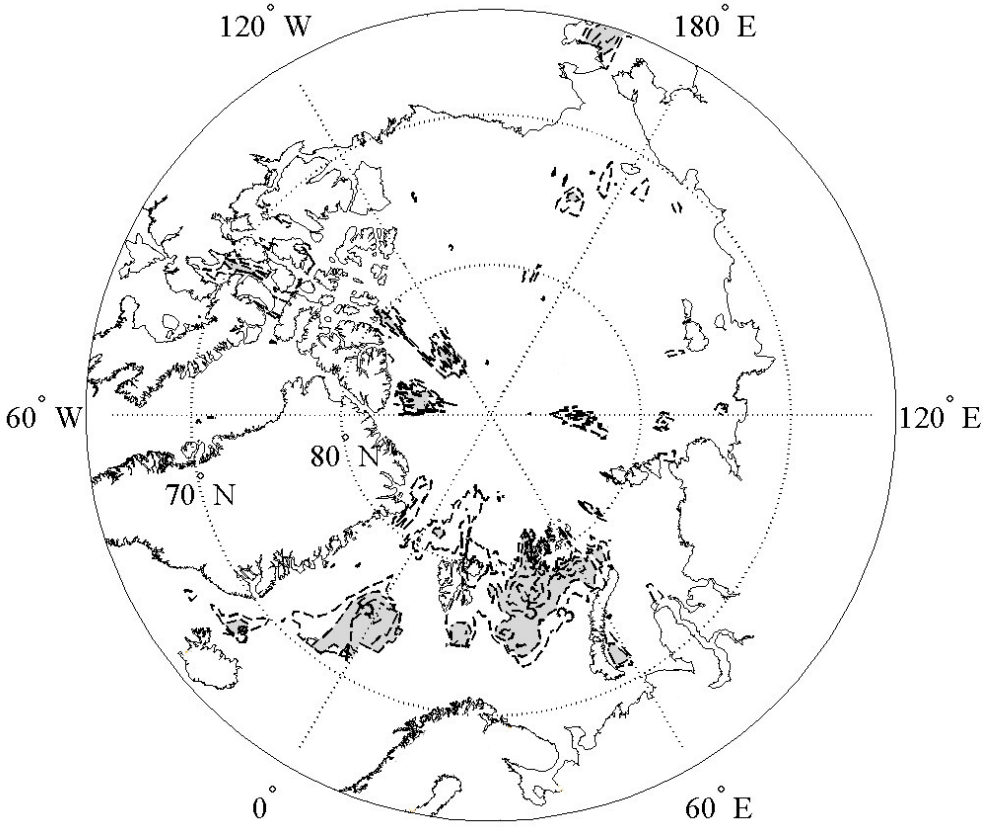

Fig. 10. As in Fig. 7 except for DJF sea ice. Grey shading indicates statistical significance at the 5% level ($r \geq |0.4|$). Sea ice data is the Reynolds ice cover data (version 2) spanning the period 1981-2001 and are available from NOAA.

Correlations between the SH and precipitation (not shown) suggest few statistically significant large-scale effects of the SH. The SH exerts the strongest influence on the precipitation in the Far East, particularly over the Sea of Japan where precipitation increases with the intensity of the SH. A stronger than usual SH is also associated with slightly enhanced precipitation over southern and Eastern Europe, which is consistent with the more active storm track.

The relationships between the SHI and meteorological variables are statistically significant in many regions over the period 1948-98. To confirm the stability of the relationships, correlation analyses have been repeated for the periods 1948-72 and 1973-98 separately and results were found to be very similar to those presented here for the whole period.

b. The SH and teleconnection patterns in the NH

A comprehensive review of NH teleconnection patterns (Panagiotopoulos *et al*. 2002) reveals that the SH is the only centre of action that is not uniquely associated with any robust teleconnection pattern in the NH. This is surprising considering the significant variability in the intensity of the SH and its non-local teleconnections with atmospheric circulation and temperature.

Multiple regression has been used to attempt to explain the SH intensity in terms of winter mean teleconnection indices obtained from Climate Prediction Center (CPC, available at http://www.cpc.ncep.noaa.gov/data/teledoc/telecontents.html). The explanatory indices are the North Atlantic Oscillation (NAO), East Atlantic (EA), Scandinavian (SCA), Polar/Eurasian (POL), West Pacific (WP), East Pacific, East Atlantic/West Russia (EA/WR) and the Pacific/North America pattern (PNA). The Arctic Oscillation (AO) index (Thomson and Wallace, 1998) has also been included (available from http://jisao.washington.edu/data/annularmodes/Data/ao_index.html).

The CPC indices are constructed by taking winter (DJF) averages of monthly standardised amplitudes of rotated principal components of monthly mean 700 hPa geopotential height anomalies for 1950-2001. Table 4 shows the results of multiple linear regression between the SHI and the teleconnection indices for DJF, and Table 5 gives cross-correlation.

The AO and WP pattern are the most significant predictors of the SH (Table 4) and this result has also been confirmed by performing stepwise selection of variables. In addition, AO and WP are the only teleconnection patterns which exhibit correlations with the SH, that are statistically significant at the 5% level (Table 5). The AO explains the most SLP variance over the NH (Thompson and Wallace, 1998), whereas the WP pattern is a dipole-shaped pattern in the West Pacific with two negatively correlated centres over the Kamchatka peninsula and the western sector of the subtropical Pacific respectively (Panagiotopoulos *et al*. 2002, not shown).

Table 4. Multiple linear regression between the SHI and time series of the main NH teleconnection patterns for the period 1950-2001. Predictors are tabulated in order of descending statistical significance.

Predictor	Coef	Std Error	p value
AO	-0.33	0.14	0.027
WP	-0.29	0.19	0.102
EP	0.25	0.21	0.237
PNA	-0.21	0.23	0.365
EA/WR	0.25	0.28	0.387
SCA	0.17	0.24	0.488
EA	-0.09	0.20	0.665

Table 5. Correlations between the SH and teleconnection patterns' indices for DJF. Correlations significant at 5% level or higher are highlighted in bold.

	SH	AO	POL	WP	EA	EP	SCA	PNA	NAO	EA/WR
SH	1	**-0.41**	**-0.40**	**0.30**	-0.23	0.18	0.17	-0.14	-0.13	-0.11
AO		1	**0.75**	0.24	0.10	-0.12	**-0.30**	-0.03	**0.68**	**0.44**
POL			1	0.19	0.03	**-0.24**	-0.17	0.18	0.06	**0.36**
WP				1	**0.43**	0.16	0.09	0.07	-0.01	0.03
EA					1	-0.09	0.18	0.21	0.14	-0.08
EP						1	0.08	-0.16	0.06	**-0.25**
SCA							1	0.07	-0.17	-0.14
PNA								1	0.09	0.19
NAO									1	0.21
EA/WR										1

Figure 11 shows the standardised DJF time series of the AO and WP amplitudes and the SHI predicted by their linear combination, which explains 21% of total SH variance. Year-to-year variations in the SH are explained moderately well by the linear combination of AO and WP pattern (Fig. 11c). It should be noted that the amount of variance in the SHI explained by these teleconnection patterns increases to 42% if time is also included in the multiple regression model because of the strong trend.

The coincidence of the unprecedented low values of the SHI in the last two decades of the 20th century with more frequent than usual El Nino episodes motivated the investigation between the SHI and the El Nino/Southern Oscillation (ENSO). The correlation between the SHI and the SO index (SOI, defined as the difference between standardised SLP at Tahiti and Darwin) was not found to be statistically significant at the 5% level.

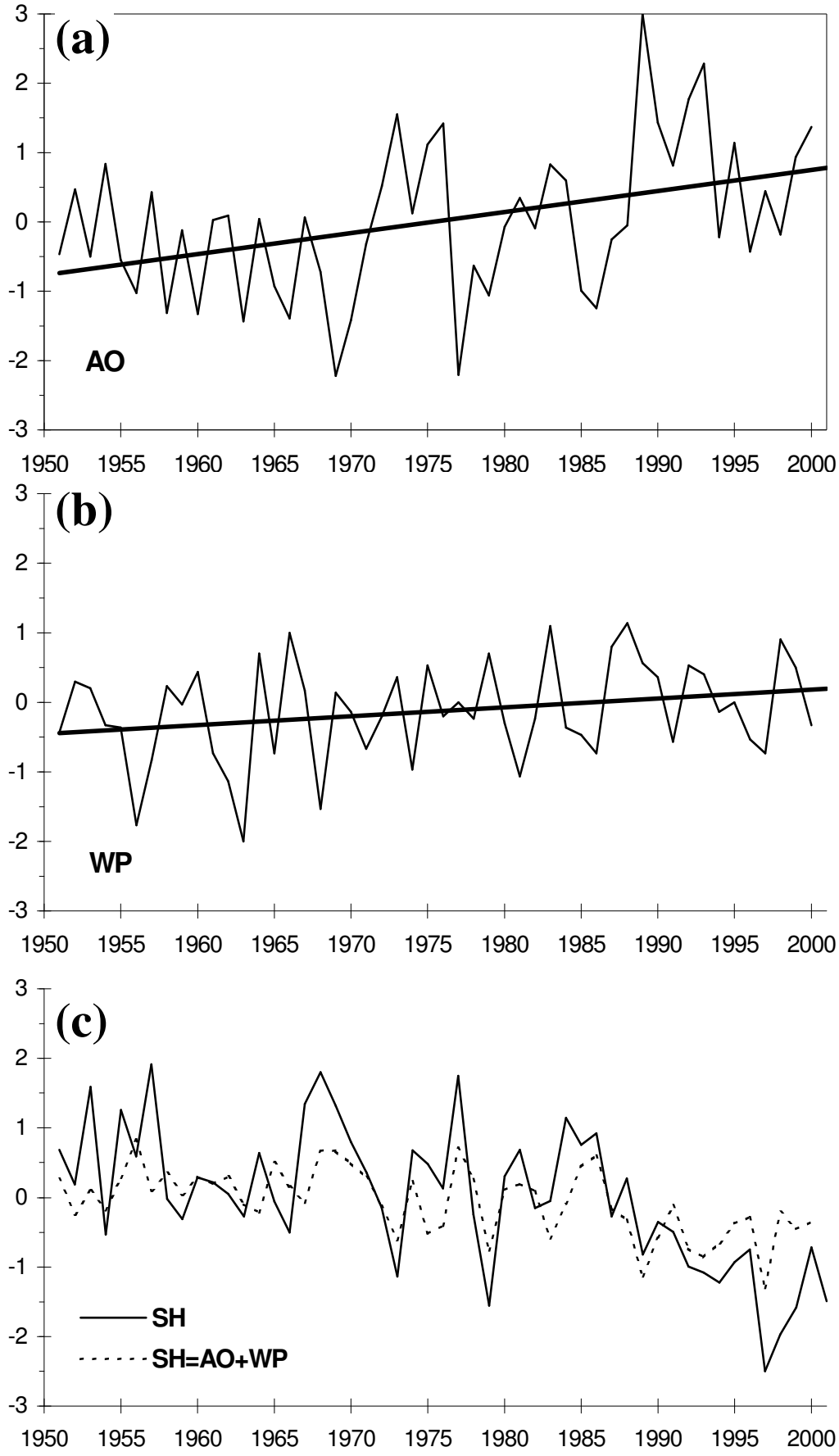

Fig. 11. Winter (DJF) standardised time series for (a) the Arctic Oscillation (AO), (b) the West Pacific (WP) pattern and (c) the observed SHI and SHI predicted from the linear combination of AO and WP.

5. Conclusions

This study has investigated variability in the intensity of the SH by carefully defining a robust SH index and then using it in correlation and regression studies of meteorological fields and teleconnection indices. The major findings are as follows:

(i) A dramatic decline in the SH exemplified by a strong downward trend of -2.5 hPa decade^{-1} in the SHI occurred between 1978 and 2001. Unprecedented low values of the SHI have been observed in this period. The weakening of the SH has also been accompanied by a slightly more westward position in the anticyclone's centre.

(ii) Correlations between the SH and various meteorological fields have shown that the SH affects atmospheric circulation and temperature patterns well outside its source area. Teleconnections between the SH and depression activity, and temperature in the western part of the Eurasian Arctic and the Mediterranean have been established. A strong link has been found between the SH intensity and sea ice formation in the western Eurasian Arctic. It has also been found that the influence of the SH in the Pacific extends farther south (into the Tropics) than was previously thought affecting convection in the equatorial western Pacific.

(iii) The SH is associated with the AO and WP patterns whose linear combination can explain year-to-year variability in the SH. AO and WP explain 21% of variance in the SH but fail to capture all of the recent trend in the SH.

While this study has answered many questions about variability in the SH and teleconnections associated with it, an important question remains: what are the reasons behind the observed decline of the SH? The possibility that the downward trend in SLP over Siberia could be an artefact of the conversion of station pressure to SLP (because of the strong surface warming) has been excluded. Major teleconnection patterns in the Northern Hemisphere explain only 21% of variance in the SH. Cohen and Entekhabi (1999), Cohen *et al*. (2001) and Saito *et al*. (2001) identified the autumn (September-November) Eurasian snow cover as a major controlling factor over the behaviour of the SH suggesting that extensive snow cover in autumn leads to a strengthening and expansion of the SH in the following winter. The suggested relationship between the SH intensity in the core region and snow cover has been re-examined using monthly snow cover data for the period 1966-99 available from NOAA (http://dss.ucar.edu/datasets/ds315.0/) but only weak positive correlations have been found between the extent of the snow cover to the south and west of Lake Baikal in October and the SHI for DJF (not shown).

Therefore, it is suggested that it is the warming observed over Siberia in recent years (IPCC, 2001) that is primarily responsible for the decline of the SH. The negative correlations between the SHI and surface temperature in Siberia are very strong with correlation coefficients of –0.66. The

observed decline in the SH intensity and increase in air temperatures occur after 1977, a period when anthropogenic global warming is believed to have started exceeding natural variability in temperature and circulation patterns (IPCC, 2001). Therefore, the observed decline in the SH may be interpreted as a signal of anthropogenic climate change. Gillett *et al.* (2003) also detected a significant influence of anthropogenic greenhouse gases and sulphate aerosols on winter SLP pointing out that the SLP response to climate change may be substantially underestimated by GCMs.

Future climate projections by GCMs also favour the argument that the decline of the SH is related to climate change by predicting a further decrease in SLP in the middle latitudes in response to increased concentrations of greenhouse gases (IPCC, 2001). A comparison of all available GCMs future projections of SLP over the source area of the SH (obtained from http://ipcc-ddc.cru.uea.ac.uk) has shown that while there is no close agreement between the models and different scenarios, a clear consensus emerges on the continuation of the observed decline of the SH until 2100 in line with increase in surface temperature. The observed rate of decline is, in fact, substantially greater than the one modelled by most GCMs suggesting that any future decline in the SH may be stronger than anticipated.

ACKNOWLEDGEMENTS

The authors gratefully acknowledge the help and interest of Prof. Brian Hoskins. Part of the analysis has been performed using Climate Explorer at Netherlands's Meteorological Institute (KNMI, available here: http://climexp.knmi.nl/). Dr Bob Livezey is also acknowledged for useful discussions.

APPENDIX

The effect of temperature on the calculation of SLP

The SLP (P_0) is computed from the station pressure P at height z by using the hydrostatic equation:

$$p(z) = p_0 e^{-\frac{z}{H}} \quad (1)$$

where p(z) is pressure at height z above mean sea level (MSL), p_0 is the pressure at z = 0, i.e. the mean sea level pressure (SLP) and H is the pressure scale height, given by $H = \frac{RT}{g}$, where R is the gas constant for dry air, T is the mean temperature of the layer and g is the global mean acceleration due to gravity at the Earth's surface.

The change in p_0 over a period of time can be calculated by differentiating (1):

$$\frac{\Delta p}{p_0} \approx \frac{\Delta p_0}{p_0}\left(1 - \frac{z}{H}\right) + \frac{z}{H}\frac{\Delta T}{T} \quad (2)$$

If it is assumed that no change took place in the station pressure p, and suitable values for the period 1920-1998 are chosen (z = 400m, T = 253K, and p_0 = 1031 hPa) then a warming (ΔT) of 3K would result in Δp_0 = -0.7 hPa compared to the observed decrease in SLP of 2.8 hPa over the same period. The corresponding value for the period 1978-98 is 0.04 hPa compared to the observed 5.2 hPa.

Using this equation, it can be estimated that a temperature rise of 16°C and 51°C would be needed to justify alone the observed decreases in SLP over the periods 1922-98 and 1978-98 respectively.

REFERENCES

Allan, R., J. Lindesay, and D. E. Parker, 1996: *El Nino Southern Oscillation and climatic variability*, CSIRO, 416 pp.

Chatfield, C., 2001: *Time-series forecasting*, Chapman and Hall, 267 pp.

Cheang, B-K., 1977: Synoptic Features and Structures of Some Equatorial Vortices over the South China Sea in the Malaysian Region during the Winter Monsoon, December 1973. *Pure Appl. Geophys.*, **115**, 1303-1334.

____, 1987: Short and long-range monsoon prediction in Southeast Asia. *Monsoons*, Fein, J. S. and P. L. Stephens. Eds., John Wiley, 579-606.

Chiyu, T., 1979: A preliminary study of low-level winds over Peninsula Malaysia during the 1967-77 North-eastern winter monsoon. *J. Met. Soc. Japan*, **57**, 354-357.

Clark, M. P., M. C. Serreze, and D. A. Robinson, 1999:. Atmospheric controls on Eurasian snow extent. *Int. J. Climatol.,* **19,** 27-40.

Cohen, J., and D. Entekhabi, 1999: Eurasian snow cover variability and Northern Hemisphere climate predictability. *Geophys. Res. Let.,* **26,** 345-348.

____, 2001: The role of the Siberian high in Northern Hemisphere climate variability. *Geophys. Res. Let.,* **28,** 299-302.

Ding, Y. 1990: Build-up, air mass transformation and propagation of Siberian high and its relations to cold surge in east Asia. *Meteorol. Atmos. Phys.,* **44,** 281-292.

Gillett, N. P., Zwiers, F. W., Weaver, A. J., and Stott, P. A., 2003: Detection of human influence on sea-level pressure. *Nature*, **422**, 292-294.

Henderson, R. 1916: Note on graduation by adjusted average. *Trans. Amer. Soc. Actuaries*, **17**, 43-48.

IPCC 2001 IPCC (2001) Climate change 2001: The scientific basis. Contribution of Working Group I to the Third Assessment Report of the Intergovernmental Panel on Climate Change (Houghton, J. T., Ding, Y., Griggs, D. J., Noguer, M., Van der Linden, P. J., Dai, X., Maskell, K. and Johnson, C. A. (Eds.)) Cambridge University Press, Cambridge and New York.

Jones, P. D., 1987: The early twentieth century Arctic High - fact or fiction? *Clim Dyn*, **1**, 63-75.

____., 1994: Hemispheric surface air temperature variations: a reanalysis and an update to 1993. *J. Climate*, **7**, 1794-1802.

Joung, C. H., and M. H. Hitchman, 1982: On the role of successive downstream development in East Asia polar air outbreaks. *Mon. Wea. Rev.,* **110**, 1224-1237.

Lydolf, P. E., 1977: *Climates of the Soviet Union*. Amsterdam Oxford: Elsevier, 443 pp.

Maslanik, J. A., M. C. Serreze, and R. G. Barry, 1996: Recent decreases in Arctic summer ice cover and linkages to atmospheric circulation anomalies. *Geophys. Res. Lett.*, **23**, 1677-1680.

Mokhov I. I., and Petukhov, V. K., 1999: Atmospheric centers of action and tendencies of their change. Izvestiya, Atmospheric and Oceanic Physics, **36**, 292-299.

Panagiotopoulos F., Shahgedanova, M., and Stephenson, D. B., 2002: A review of Northern Hemisphere winter-time teleconnection patterns. *J. Phys. IV*, **12**, (2002).

Przybylak, R., 2000: Temporal and spatial variation of surface air temperature over the period of instrumental observations in the Arctic. *J. Climate*, **20**, 587-614.

Rogers, J. C., 1997: North Atlantic storm track variability and its association to the north Atlantic oscillation and climate variability of northern Europe. *J. Climate*, **10**, 1635-1647.

____, and Mosley-Thompson, E., 1995: Atlantic Arctic cyclones and the mild Siberian winters of the 1980s. *Geophys. Res. Lett.*, **22**, 799-802.

Sahsamanoglou, H. S., Makrogiannis, T. J., and Kallimopoulos, P. P., 1991. Some aspects of the basic characteristics of the Siberian anticyclone. *Int. J. Climatol.,* **11,** 827-839.

Saito, K., Cohen, J., and Entekhabi, D., 2001: Evolution of atmospheric response to early-season Eurasian snow cover anomalies. *Mon. Wea. Rev.,* **129**, 2746-2760.

Stephenson, D. B., Wanner, H., Brönnimann, S., and Luterbacher J., 2002: The history of scientific research on the North Atlantic Oscillation. *The North Atlantic Oscillation*: *Climate Significance and Environmental Impact,* J. W. Hurrell, Y. Kushnir, G. Ottersen, and M. Visbeck, Eds., *Geophys. Monogr.*, No. 134, Amer. Geophys. Union, 37-50.

Thompson, D. W. J., and Wallace, J. M., 1998: The Arctic Oscillation signature in the wintertime geopotential height and temperature fields. *Geophys. Res. Let.,* **25,** 1297-1300.

Trenberth, K. E., and. Paolino., D. A., 1980: The Northern Hemisphere sea-level pressure data set: Trends, errors, and discontinuities. *Mon. Wea. Rev.,* **108,** 855-872.

Walsh, J. E., Chapman, W. L., and Shy, T. L. 1996: Recent decrease of sea level pressure in the central Arctic. *J. Climate*, **9**, 480-485.